

Coupled buffeting response analysis of long-span bridges by the CQC approach

Quanshun Ding[†], Airong Chen[‡] and Haifan Xiang^{‡†}

State Key Lab for Disaster Reduction in Civil Engineering, Tongji University, Shanghai 200092, China

(Received January 24, 2001, Accepted March 13, 2002)

Abstract. Based on the modal coordinates of the structure, a finite-element and CQC (complete quadratic combination) method for analyzing the coupled buffeting response of long-span bridges is presented. The formulation of nodal equivalent aerodynamic buffeting forces is derived based on a reasonable assumption. The power spectral density and variance of nodal displacements and elemental internal forces of the bridge structure are computed using the finite-element method and the random vibration theory. The method presented is very efficient and can consider the arbitrary spectrum and spatial coherence of natural winds and the multimode and intermode effects on the buffeting responses of bridge structures. A coupled buffeting analysis of the Jiangyin Yangtse River Suspension Bridge with 1385 m main span is performed as an example. The results analyzed show that the multimode and intermode effects on the buffeting response of the bridge deck are quite remarkable.

Key words: long-span bridges; aerodynamic coupling; buffeting analysis; finite-element and CQC method; multimode and intermode; Jiangyin Yangtse River Suspension Bridge.

1. Introduction

Natural winds are turbulent in nature. Buffeting is an aerodynamic random vibration of bridge structures due to the wind fluctuation. The buffeting response of a bridge deck increases considerably as the main span of the bridge lengthens. The buffeting response also appears within a wide range of wind speeds and lasts for almost the whole design life of the bridge. Thus, frequent occurrence of buffeting response of relatively large amplitude may influence the endurance of structure and cause fatigue damage to the bridge components. Therefore, aerodynamic design must ensure that the bridge does not vibrate excessively under gusty winds.

To the writers' knowledge, Davenport (1961, 1962) first applied statistical concepts to the buffeting analysis of structures and suggested the aerodynamic admittance to reduce the error caused by the quasi-steady forces. However, the aerodynamic stiffness and coupling effects among modes were neglected. Scanlan (Scanlan and Gade 1977, Scanlan 1978, Scanlan and Jones 1990) proposed a basic theory for multimode buffeting analysis of long-span bridges which the self-excited forces were taken into consideration. Chen (1993) utilized the characteristics of the two approaches and

[†] Lecturer
[‡] Professor
^{‡†} Senior Professor

presented a response-spectrum method for the buffeting response analysis of long-span bridges.

For the buffeting response analysis of long-span bridges, the conventional mode-by-mode approach is widely used. Matsumoto *et al.* (1994) pointed out the importance of aerodynamic coupling among modes of vibration when estimating the buffeting response, particularly at higher wind velocities. Jain *et al.* (1996) considered both multimode and intermode buffeting response using the random vibration-based mode superposition method in the frequency domain. Katsuchi *et al.* (1999) refined this frequency domain approach and applied it to the Akashi-Kaikyo Bridge, which is the longest suspension bridge built in the world so far. This approach only considers the aerodynamic forces on the bridge deck and the computational efforts of the dual integral are usually large. Xu (1998) combined the finite element method and the pseudo-excitation approach in the computation of the buffeting response of a bridge. Chen (2000) investigated the effects of aerodynamic coupling among modes of vibration on the buffeting response of long-span bridges. Although the time-domain buffeting analysis is also developed recently (Minh *et al.* 1999, Chen *et al.* 2000, Cao 1999), the frequency-domain method is more attractive and widely applied for its simplicity and efficiency.

This paper describes a method similar to Chen (2000) with some details and revisions. Based on the modal coordinates of the structure, a finite-element and CQC (complete quadratic combination) method for analyzing the coupled buffeting response of long-span bridges is presented. The formulation of nodal equivalent aerodynamic buffeting forces is derived based on a reasonable assumption. The power spectral density and variance of nodal displacements and elemental internal forces of bridge structures are computed using the finite-element method and the random vibration theory. Moreover, a coupled buffeting analysis of Jiangyin Yangtse River Suspension Bridge with 1385 m main span is performed as an example.

2. Equation of motion

The governing equation of motion of a bridge structure excited by aerodynamic forces is given in a matrix form by

$$\mathbf{M}\ddot{\mathbf{X}} + \mathbf{C}\dot{\mathbf{X}} + \mathbf{K}\mathbf{X} = \mathbf{F}_{se} + \mathbf{F}_b \quad (1)$$

where \mathbf{M} , \mathbf{C} , and \mathbf{K} = structural mass, damping, stiffness matrices, respectively; \mathbf{X} , $\dot{\mathbf{X}}$, $\ddot{\mathbf{X}}$ = nodal displacement, velocity, and acceleration vector; \mathbf{F} indicates the nodal equivalent force vector, and the subscripts *se* and *b* represent the self-excited and turbulence-induced buffeting force components, respectively.

For the harmonic motion, the self-excited forces per unit span are expressed in Scanlan's extended format below (Scanlan 1978, 1993):

$$L_{se}(t) = \frac{1}{2}\rho U^2(2B)\left(KH_1^*\frac{\dot{h}}{U} + KH_2^*\frac{B\dot{\alpha}}{U} + K^2H_3^*\alpha + K^2H_4^*\frac{h}{B} + KH_5^*\frac{\dot{p}}{U} + K^2H_6^*\frac{p}{B}\right) \quad (2a)$$

$$D_{se}(t) = \frac{1}{2}\rho U^2(2B)\left(KP_1^*\frac{\dot{p}}{U} + KP_2^*\frac{B\dot{\alpha}}{U} + K^2P_3^*\alpha + K^2P_4^*\frac{p}{B} + KP_5^*\frac{\dot{h}}{U} + K^2P_6^*\frac{h}{B}\right) \quad (2b)$$

$$M_{se}(t) = \frac{1}{2}\rho U^2(2B^2)\left(KA_1^*\frac{\dot{h}}{U} + KA_2^*\frac{B\dot{\alpha}}{U} + K^2A_3^*\alpha + K^2A_4^*\frac{h}{B} + KA_5^*\frac{\dot{p}}{U} + K^2A_6^*\frac{p}{B}\right) \quad (2c)$$

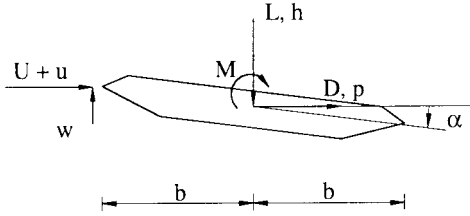


Fig. 1 Displacements and forces on bridge section

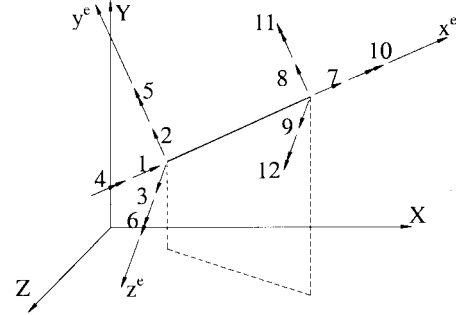


Fig. 2 Directions of 12-DOF frame member

where ρ = air density; U = mean wind velocity; $B = 2b$ = bridge deck width; $K = \omega B/U$ = reduced frequency, ω = circular frequency of vibration; h , p , and α = vertical, lateral, and torsional displacements, respectively; the over-dot denotes the partial differentiation with respect to time t ; and H_i^* , P_i^* , A_i^* ($i = 1 \sim 6$) = non-dimensional flutter derivatives, which are functions of the reduced frequency and depend on the geometrical configuration of the bridge section and the approach flow. The aerodynamic forces and the displacements are shown in Fig. 1.

The expressions (2) are the real-number form of self-excited forces. In complex notation, the corresponding expressions of self-excited forces read (Starossek 1998)

$$L_{se}(t) = \omega^2 \rho B^2 (C_{Lh} h + C_{Lp} p + BC_{L\alpha} \alpha) \quad (3a)$$

$$D_{se}(t) = \omega^2 \rho B^2 (C_{Dh} h + C_{Dp} p + BC_{D\alpha} \alpha) \quad (3b)$$

$$M_{se}(t) = \omega^2 \rho B^2 (BC_{Mh} h + BC_{Mp} p + B^2 C_{M\alpha} \alpha) \quad (3c)$$

where C_{rs} ($r = D, L, M$; $s = h, p, \alpha$) = complex coefficients of self-excited forces.

The relationships between real and complex aerodynamic coefficients can be established by comparing the corresponding self-excited force expressions. The following relations are found:

$$C_{Lh} = H_4^* + iH_1^*, \quad C_{Lp} = H_6^* + iH_5^*, \quad C_{L\alpha} = H_3^* + iH_2^* \quad (4a)$$

$$C_{Dh} = P_6^* + iP_5^*, \quad C_{Dp} = P_4^* + iP_1^*, \quad C_{D\alpha} = P_3^* + iP_2^* \quad (4b)$$

$$C_{Mh} = A_4^* + iA_1^*, \quad C_{Mp} = A_6^* + iA_5^*, \quad C_{M\alpha} = A_3^* + iA_2^* \quad (4c)$$

In the FEM analysis, the distributed forces of the bridge deck are converted into nodal equivalent forces at member ends as follows:

$$F_{se}^e = \omega^2 A_{se}^e X^e \quad (5)$$

where $A_{se}^e = 12$ by 12 self-excited force matrix of the member; the subscript e represents the local coordinates of the member (see Fig. 2). The lumped self-excited force matrix of a bridge deck member with L length is

$$\mathbf{A}_{se}^e = \begin{bmatrix} \mathbf{A}_1 & \mathbf{0} \\ \mathbf{0} & \mathbf{A}_1 \end{bmatrix} \quad (6)$$

where

$$\mathbf{A}_1 = \frac{1}{2}\rho B^2 L \begin{bmatrix} 0 & 0 & 0 & 0 & 0 & 0 \\ 0 & C_{Lh} & C_{Lp} & BC_{L\alpha} & 0 & 0 \\ 0 & C_{Dh} & C_{Dp} & BC_{D\alpha} & 0 & 0 \\ 0 & BC_{Mh} & BC_{Mp} & B^2 C_{M\alpha} & 0 & 0 \\ 0 & 0 & 0 & 0 & 0 & 0 \\ 0 & 0 & 0 & 0 & 0 & 0 \end{bmatrix} \quad (7)$$

Since the self-excited forces are non-conservative, the self-excited force matrix of the member is generally asymmetrical and is a function of reduced frequency. When these matrices of the members are converted into the global coordinates and are assembled, then

$$\mathbf{F}_{se} = \omega^2 \mathbf{A}_{se} \mathbf{X} \quad (8)$$

where \mathbf{A}_{se} = self-excited force matrix of the structure. Obviously, \mathbf{A}_{se} is a complex matrix.

The buffeting forces per unit span on bridge structures due to wind fluctuations are given by Davenport (1962) and Scanlan (1978, 1993):

$$L_b = \frac{1}{2}\rho U^2 B \left[2C_L \chi_{Lu} \frac{u'}{U} + (C'_L + C_D) \chi_{Lw} \frac{w'}{U} \right] \quad (9a)$$

$$D_b = \frac{1}{2}\rho U^2 B \left[2C_D \chi_{Du} \frac{u'}{U} + C'_D \chi_{Dw} \frac{w'}{U} \right] \quad (9b)$$

$$M_b = \frac{1}{2}\rho U^2 B^2 \left[2C_M \chi_{Mu} \frac{u'}{U} + C'_M \chi_{Mw} \frac{w'}{U} \right] \quad (9c)$$

where C_L , C_D , and C_M = static lift, drag, and moment coefficients (referred to deck width B), respectively; $C'_L = dC_L/d\alpha$, $C'_D = dC_D/d\alpha$, and $C'_M = dC_M/d\alpha$; χ_{Lu} , χ_{Lw} , χ_{Du} , χ_{Dw} , χ_{Mu} , χ_{Mw} = aerodynamic admittance functions, which are functions of reduced frequency and dependent on the geometrical configuration of the bridge section; and u' and w' = two components of wind fluctuations on the local coordinates of the member. It is assumed here that the member is located on the plane perpendicular to the longitudinal wind velocity. Thus $u' = u$, $w' = w \cos \theta$, where u and w are the longitudinal and vertical wind fluctuations, respectively, and θ is the angle between the local axis x^e and the global axis X .

The aerodynamic buffeting forces aforementioned can be expressed as below

$$\mathbf{P}_b = 0.5\rho U (C_{bu}u + C_{bw}w) \quad (10)$$

where

$$\mathbf{P}_b = \begin{Bmatrix} L_b \\ D_b \\ M_b \end{Bmatrix}, \quad \mathbf{C}_{bu} = B \begin{Bmatrix} 2C_L \\ 2C_D \\ 2BC_M \end{Bmatrix}, \quad \mathbf{C}_{bw} = B \cos \theta \begin{Bmatrix} C'_L + C_D \\ C'_D \\ BC'_M \end{Bmatrix}$$

When the member is small enough, it can be assumed approximately that the longitudinal and vertical wind fluctuations are distributed linearly on the member, then

$$\mathbf{u} = \begin{bmatrix} 1 - \frac{x}{L} & \frac{x}{L} \end{bmatrix} \begin{Bmatrix} u_1 \\ u_2 \end{Bmatrix} = \mathbf{A} \mathbf{u}^e \quad (11a)$$

$$\mathbf{w} = \begin{bmatrix} 1 - \frac{x}{L} & \frac{x}{L} \end{bmatrix} \begin{Bmatrix} w_1 \\ w_2 \end{Bmatrix} = \mathbf{A} \mathbf{w}^e \quad (11b)$$

where x and L = axial location and length of the member, respectively; and the subscripts 1 and 2 indicate the two ends of the member.

The consistent buffeting forces at the member ends in the local coordinate system can be obtained by the following definite integral:

$$\begin{aligned} \mathbf{F}_b^e &= \int_L \mathbf{B}^T \mathbf{P}_b dx \\ &= 0.5 \rho U \left(\int_L \mathbf{B}^T \mathbf{C}_{bu} \mathbf{A} dx \mathbf{u}^e + \int_L \mathbf{B}^T \mathbf{C}_{bw} \mathbf{A} dx \mathbf{w}^e \right) \\ &= 0.5 \rho U (\mathbf{A}_{bu}^e \mathbf{u}^e + \mathbf{A}_{bw}^e \mathbf{w}^e) \end{aligned} \quad (12)$$

where \mathbf{A}_{bu}^e and \mathbf{A}_{bw}^e = buffeting force matrices of the member corresponding to the longitudinal and vertical wind fluctuations, respectively; \mathbf{B} = matrix of interpolated functions

$$\mathbf{B} = \begin{bmatrix} 0 & -N_1 & 0 & 0 & 0 & -N_3 & 0 & -N_2 & 0 & 0 & 0 & N_4 \\ 0 & 0 & -N_1 & 0 & N_3 & 0 & 0 & 0 & -N_2 & 0 & -N_4 & 0 \\ 0 & 0 & 0 & -N_5 & 0 & 0 & 0 & 0 & 0 & -N_6 & 0 & 0 \end{bmatrix} \quad (13)$$

where the functions: $N_1 = 1 - 3\left(\frac{x}{L}\right)^2 + 2\left(\frac{x}{L}\right)^3$; $N_2 = 3\left(\frac{x}{L}\right)^2 - 2\left(\frac{x}{L}\right)^3$; $N_3 = x\left(1 - \frac{x}{L}\right)^3$;

$$N_4 = \frac{x^2}{L}\left(1 - \frac{x}{L}\right); \quad N_5 = 1 - \frac{x}{L}; \quad N_6 = \frac{x}{L}$$

Inserting Eq. (13) into Eq. (12) and integrating, yields

$$\mathbf{A}_{bu}^e = \frac{-BL}{30} \begin{bmatrix} 0 & 21C_L & 21C_D & 20BC_M & -3LC_D & 3LC_L & 0 & 9C_L & 9C_D & 10BC_M & 2LC_D & -2LC_L \\ 0 & 9C_L & 9C_D & 10BC_M & -2LC_D & 2LC_L & 0 & 21C_L & 21C_D & 20BC_M & 3LC_D & -3LC_L \end{bmatrix}^T$$

$$\mathbf{A}_{bw}^e = \frac{-BL\cos\theta}{60} \begin{bmatrix} 0 & 21(C'_L + C_D) & 21C'_D & 20BC'_M & -3LC'_D & 3L(C'_L + C_D) \\ 0 & 9(C'_L + C_D) & 9C'_D & 10BC'_M & -2LC'_D & 2L(C'_L + C_D) \\ 0 & 9(C'_L + C_D) & 9C'_D & 10BC'_M & 2LC'_D & -2L(C'_L + C_D) \\ 0 & 21(C'_L + C_D) & 21C'_D & 20BC'_M & 3LC'_D & -3L(C'_L + C_D) \end{bmatrix}^T$$

The nodal local buffeting forces expressed by Eq. (12) can be converted into the global coordinate system using the coordinate transformation matrix. As a result, the nodal global buffeting force vector can be obtained as

$$\mathbf{F}_b = 0.5\rho U(\mathbf{A}_{bu}\mathbf{u} + \mathbf{A}_{bw}\mathbf{w}) \quad (14)$$

where \mathbf{A}_{bu} and \mathbf{A}_{bw} = global buffeting force matrices; and \mathbf{u} and \mathbf{w} = the r -row nodal fluctuating wind vectors for the longitudinal and vertical components, respectively, where r is the number of nodes subjected to wind fluctuations.

Apart from the bridge deck, the buffeting forces also act on the bridge towers, cables, and other components. It is therefore desirable to have a buffeting analysis of the whole bridge other than the bridge deck only. Besides the bridge deck, these formulae above are suitable to other bridge components, and hence the method presented could be applied to examine interactions between bridge components.

3. Multimode buffeting analysis

Based on the preceding part, the governing equations of motion of the bridge structure are given as

$$\mathbf{M}\ddot{\mathbf{X}} + \mathbf{C}\dot{\mathbf{X}} + \mathbf{K}\mathbf{X} - \omega^2\mathbf{A}_{se}\mathbf{X} = \mathbf{F}_b \quad (15)$$

It is assumed that the buffeting response of the bridge structure can be approximately expressed by the first m structural natural modes as

$$\mathbf{X} = \Phi\mathbf{q} \quad (16)$$

where Φ = n -row by m -column matrix of natural modes, can be provided by the dynamic characteristic analysis in the loaded state; \mathbf{q} = m -row vector of generalized coordinates; and n = total number of degrees of freedom. Inserting Eq. (16) into Eq. (15) and multiplying by Φ^T on the left yields

$$\ddot{\mathbf{q}} + \bar{\mathbf{C}}\dot{\mathbf{q}} + \Lambda\mathbf{q} - \omega^2\bar{\mathbf{A}}_{se}\mathbf{q} = \mathbf{Q}_b \quad (17)$$

where Λ = diagonal eigenvalue matrix from the dynamic characteristic analysis; $\bar{\mathbf{C}} = \Phi^T\mathbf{C}\Phi$ and $\bar{\mathbf{A}}_{se} = \Phi^T\mathbf{A}_{se}\Phi$; $\mathbf{Q}_b = (\bar{\mathbf{A}}_{bu}\mathbf{u} + \bar{\mathbf{A}}_{bw}\mathbf{w})$ (where $\bar{\mathbf{A}}_{bu} = \Phi^T\mathbf{A}_{bu}$ and $\bar{\mathbf{A}}_{bw} = \Phi^T\mathbf{A}_{bw}$) = generalized buffeting force vector.

In terms of the random vibration theory, the power spectral density (PSD) matrices of the vectors

of generalized modal response \mathbf{q} and nodal displacement \mathbf{X} are obtained by

$$\mathbf{S}_q(\omega) = \mathbf{H}^*(\omega)\mathbf{S}_{Q_b}(\omega)\mathbf{H}^T(\omega) \quad (18)$$

$$\mathbf{S}_X(\omega) = \mathbf{\Phi}\mathbf{H}^*(\omega)\mathbf{S}_{Q_b}(\omega)\mathbf{H}^T(\omega)\mathbf{\Phi}^T \quad (19)$$

where $\mathbf{H}(\omega)$ = transfer function matrix.

$$\mathbf{H}(\omega) = [-\omega^2(\mathbf{I} + \bar{\mathbf{A}}_{se}) + i\omega\bar{\mathbf{C}} + \mathbf{\Lambda}]^{-1} \quad (20)$$

and \mathbf{I} = unit matrix; the subscript * and T denote the complex conjugate and transpose, respectively.

Because of the aerodynamic coupling among modes of vibration, the off-diagonal components of matrix generally have nonzero values depending on the dynamic and aerodynamic characteristics of the bridge. These components may strongly influence the buffeting response as the wind velocity increases.

The PSD matrix of the generalized buffeting forces is given by:

$$\mathbf{S}_{Q_b}(\omega) = \mathbf{S}_{Q_b}^{(1)}(\omega) + \mathbf{S}_{Q_b}^{(2)}(\omega) \quad (21)$$

$$\mathbf{S}_{Q_b}^{(1)}(\omega) = 0.25\rho^2 U^2 (\bar{\mathbf{A}}_{bu}\mathbf{S}_{uu}\bar{\mathbf{A}}_{bu}^T + \bar{\mathbf{A}}_{bw}\mathbf{S}_{ww}\bar{\mathbf{A}}_{bw}^T)$$

$$\mathbf{S}_{Q_b}^{(2)}(\omega) = 0.25\rho^2 U^2 (\bar{\mathbf{A}}_{bu}\mathbf{S}_{uw}\bar{\mathbf{A}}_{bw}^T + \bar{\mathbf{A}}_{bw}\mathbf{S}_{wu}\bar{\mathbf{A}}_{bu}^T)$$

where \mathbf{S}_{uu} and \mathbf{S}_{ww} = PSD matrices of \mathbf{u} and \mathbf{w} components, respectively; $\mathbf{S}_{uw} = \mathbf{S}_{wu}^*$ = cross-spectral density (CSD) matrices between the \mathbf{u} and \mathbf{w} components, and $\mathbf{S}_{uw}(\omega) = \mathbf{C}_{uw}(\omega) + i\mathbf{Q}_{uw}(\omega)$, with \mathbf{C}_{uw} and \mathbf{Q}_{uw} being the cospectra and quadrature spectra, respectively. $\mathbf{S}_{Q_b}^{(1)}(\omega)$ is induced by the PSD matrices of \mathbf{u} and \mathbf{w} components and $\mathbf{S}_{Q_b}^{(2)}(\omega)$ reflects the effects of the CSD matrices between \mathbf{u} and \mathbf{w} components. It has been noted that the difference of positive directions of the longitudinal and vertical wind fluctuations can change the sign of $\mathbf{S}_{Q_b}^{(2)}(\omega)$ and it is associated with the static wind coefficients. Therefore, it is necessary to divide the PSD matrix of the generalized buffeting forces into two parts to analyze the buffeting response.

The power spectra of the wind components u and w in the atmospheric boundary layer, expressed as functions of ω , are (Simiu and Scanlan 1986)

$$S_{uu}(\omega) = \frac{200u_*^2 z}{2\pi U(z) \left[1 + 50 \frac{\omega z}{2\pi U(z)} \right]^{5/3}}, \quad S_{ww}(\omega) = \frac{3.36u_*^2 z}{2\pi U(z) \left[1 + 10 \left(\frac{\omega z}{2\pi U(z)} \right)^{5/3} \right]} \quad (22a,b)$$

where z = elevation above ground; u_* = friction velocity, is a function of the surface roughness; and $U(z)$ = wind velocity at height z . An empirical formula for the cospectrum, \mathbf{C}_{uw} , similar in form to the autospectra and suitable for engineering application (Kaimal *et al.* 1972, Jones *et al.* 1992), is

$$\mathbf{C}_{uw}(\omega) = \frac{14u_*^2 z}{2\pi U(z) \left[1 + 9.6 \left(\frac{\omega z}{2\pi U(z)} \right)^{2.4} \right]} \quad (23)$$

No quantitative assessment of the quadrature spectrum Q_{uw} has yet been made (Jones *et al.* 1992, Panofsky and Dutton 1984).

The spanwise cross-spectral densities of the wind components are expressed in conventional form as (Simiu and Scanlan 1986)

$$S_{uu}(r, \omega) = \sqrt{S_{uu}(z_1, \omega)S_{uu}(z_2, \omega)} e^{-\hat{f}_u} \quad (24)$$

$$S_{ww}(r, \omega) = S_{ww}(z, \omega) e^{-\hat{f}_w} \quad (25)$$

$$\hat{f}_u = \frac{\omega [C_z^2(z_1 - z_2)^2 + C_y^2(y_1 - y_2)^2]^{1/2}}{2\pi \frac{1}{2}[U(z_1) + U(z_2)]}, \quad \hat{f}_w = \frac{\omega C_w |y_1 - y_2|}{2\pi U(z)} \quad (26)$$

where y_1, y_2 and z_1, z_2 = the spanwise and vertical coordinates of the two points; C_z and C_y = the decay factors of the vertical and spanwise coherence of longitudinal wind fluctuation, and C_w = the decay factor of the coherence of vertical wind fluctuation, are suggested as 10, 16, and 8 (Simiu and Scanlan 1986), respectively.

From Eqs. (18) and (19), the components of $S_q = S_q^{(1)} + S_q^{(2)}$ and $S_X = S_X^{(1)} + S_X^{(2)}$ matrices can be expressed as

$$S_{q_{ij}}^{(r)}(\omega) = \sum_{k=1}^m \sum_{l=1}^m H_{ik}^*(\omega) S_{Q_{kl}}^{(r)}(\omega) H_{jl}(\omega) \quad (27)$$

$$S_{X_i}^{(r)}(\omega) = \sum_{k=1}^m \sum_{l=1}^m \phi_{ik} S_{q_{kl}}^{(r)}(\omega) \phi_{il} \quad (28)$$

where $r = 1$ or 2 . Thus the variances of the generalized modal responses and nodal displacements are given by

$$\sigma_{q_{ii}}^2 = \int_0^\infty (S_{q_{ii}}^{(1)}(\omega) + |S_{q_{ii}}^{(2)}(\omega)|) d\omega \quad (29)$$

$$\begin{aligned} \sigma_{X_i}^2 &= \int_0^\infty (S_{X_i}^{(1)}(\omega) + |S_{X_i}^{(2)}(\omega)|) d\omega \\ &= \sum_{k=1}^m \sum_{l=1}^m \phi_{ik} \left(\int_0^\infty (S_{q_{kl}}^{(1)}(\omega) + |S_{q_{kl}}^{(2)}(\omega)|) d\omega \right) \phi_{il} \end{aligned} \quad (30)$$

when the static wind coefficients of bridge deck sections or the positive directions of the longitudinal and vertical wind fluctuations vary, the sign of the PSDs of the generalized modal responses and nodal displacements caused by the CSDs between the \mathbf{u} and \mathbf{w} components may be different. Thus, the absolute values are used in these formulae.

Based on the PSDs of nodal displacements, the PSDs of elemental internal forces of the bridge structure can be determined. The determinant relationship between the elemental internal forces and nodal displacements is

$$\mathbf{P}^e = \mathbf{K}^e \mathbf{X}^e = \mathbf{K}^e \mathbf{T}^e \mathbf{X}_1 \quad (31)$$

where \mathbf{P}^e = elemental internal force vector; \mathbf{K}^e = elemental stiffness matrix; \mathbf{T}^e = global-to-local coordinate transformation matrix; \mathbf{X}^e = nodal displacement vector in the elemental local coordinates; \mathbf{X}_1 = nodal displacement vector in the structural global coordinates related to the element.

Denoting $\mathbf{G} = \mathbf{K}^e \mathbf{T}^e$, then the PSD matrices of the elemental internal forces are

$$\mathbf{S}_p^{(r)}(\omega) = \mathbf{G} \mathbf{S}_{X_1}^{(r)}(\omega) \mathbf{G}^T \quad (r = 1, 2) \quad (32)$$

where $\mathbf{S}_{X_1}^{(r)}(\omega)$ ($r = 1, 2$) = PSD matrices of the nodal displacement vector \mathbf{X}_1 . Once the PSDs of the elemental internal forces are obtained, both the variances and RMS values can be determined similar to the nodal displacement.

When the CSDs between different generalized buffeting forces are negligible in comparison with the PSD, $\mathbf{S}_{Q_{b_{ij}}}^{(r)}(\omega)$, i.e., $\mathbf{S}_{Q_{b_{ij}}}^{(r)}(\omega) = 0$ ($i \neq j$), the components of $\mathbf{S}_q(\omega)$ become

$$\mathbf{S}_{q_{ij}}^{(r)}(\omega) = \sum_{k=1}^m H_{ik}^*(\omega) S_{Q_{b_{kk}}}^{(r)}(\omega) H_{jk}(\omega) \quad (33)$$

When the aerodynamic coupling among vibration modes is neglected, i.e., the non-diagonal elements of \mathbf{A}_{se} are taken as zero and $H_{ij}(\omega) = 0$ ($i \neq j$), then $\mathbf{S}_{q_{ij}}^{(r)}(\omega)$ ($r = 1, 2$) is given as

$$\mathbf{S}_{q_{ij}}^{(r)}(\omega) = H_{ii}^*(\omega) S_{Q_{b_{ij}}}^{(r)}(\omega) H_{jj}(\omega) \quad (34)$$

When both $\mathbf{S}_{Q_{b_{ij}}}^{(r)}(\omega) = 0$ ($i \neq j$) and the aerodynamic coupling among vibration modes are neglected, the following expression is obtained:

$$\mathbf{S}_{q_{ii}}^{(r)}(\omega) = |H_{ii}(\omega)|^2 \mathbf{S}_{Q_{b_{ii}}}^{(r)}(\omega); \quad \mathbf{S}_{q_{ij}}^{(r)}(\omega) = 0 \quad (i \neq j, r = 1, 2) \quad (35)$$

For the purpose of evaluating the response in the multimode sense from single-mode response, the square-root of the sum of square (SRSS) of single-mode responses is used, i.e.,

$$SRSS(X_i) = \sqrt{\sigma_{X_{i,1}}^2 + \sigma_{X_{i,2}}^2 + \dots + \sigma_{X_{i,m}}^2} \quad (36)$$

where m = the number of natural modes

4. Example

To illustrate the reliability and effectiveness of the method presented and the analyzing software, numerical buffeting analysis has been performed on two typical examples: a simply supported beam structure with a thin-plate section and Jiangyin Yangtse River Suspension Bridge.

4.1 A simply supported beam structure

The first example considered is that of a simply supported beam structure with a thin-plate section and it mainly serves as a check on the method presented. The structural properties are given as follows: span $L = 300$ m; width $B = 40$ m; vertical bending stiffness $EI_z = 2.1 \times 10^6$ Mpa · m⁴; lateral bending stiffness $EI_y = 1.8 \times 10^7$ Mpa · m⁴; torsional stiffness $GI_t = 4.1 \times 10^5$ Mpa · m⁴;

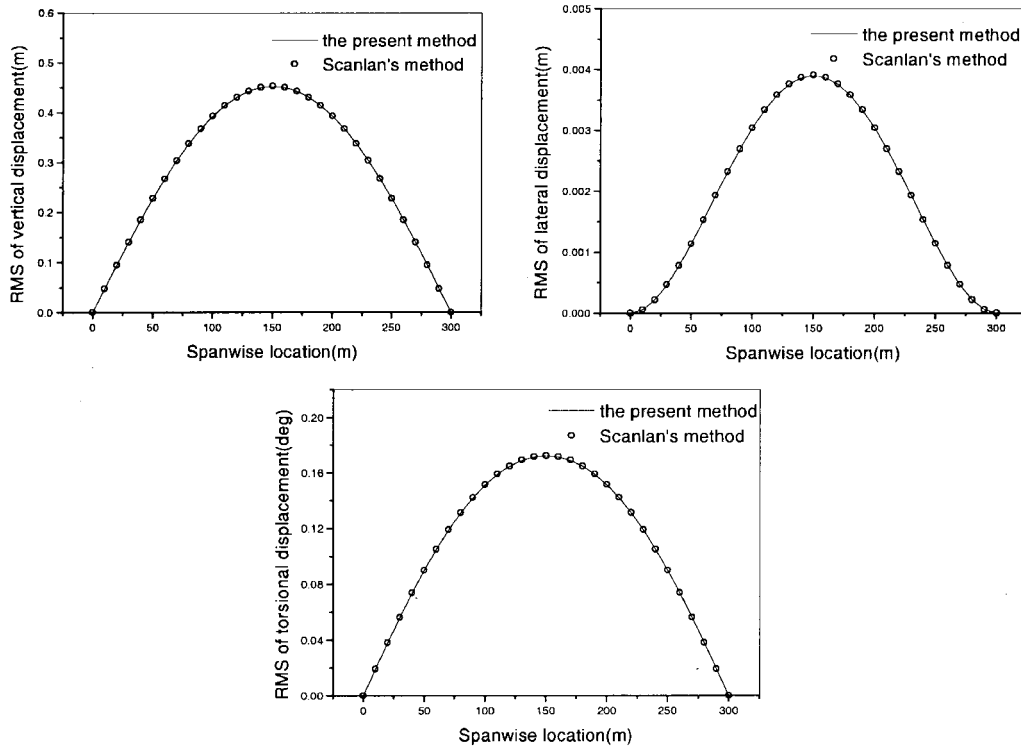


Fig. 3 Comparison of the RMS values of displacement buffeting responses at the span center

mass $m = 20,000 \text{ kg/m}$; mass moment of inertia $I_m = 4.5 \times 10^6 \text{ kg} \cdot \text{m}^2/\text{m}$; and air mass density $\rho = 1.25 \text{ kg/m}^3$. The structural damping ratio for each natural mode is assumed to 0.005.

The self-excited aerodynamic lift and moment acting on the thin-plate section can be represented approximately by Theodorsen's function, and the flutter derivatives H_i^* and A_i^* ($i = 1 \sim 4$) can be determined from Theodorsen's function (Scanlan 1993). The static wind coefficients of the section at the zero attack angle are taken as $C_L = 0.128$, $C_D = 0.0697$, $C_M = -0.0074$, $dC_L/d\alpha = -5.5577$, $dC_D/d\alpha = 0.0$, $dC_M/d\alpha = 1.2662$. The simply supported beam is divided into 30 elements. The first 20 natural modes of the structure are computed, which are used in the buffeting analysis. Both the present method and method of Scanlan and his coworkers are applied to analyze the coupled buffeting response problem. The comparison of the RMS values of displacement buffeting responses at the span center is shown as Fig. 3 at the mean wind velocity of 40 m/s. It can be seen that the results of the present method have very good agreement with those of the Scanlan's method.

4.2 Jianguyin Yangtse River Suspension Bridge

The coupled buffeting analysis of the Jianguyin Yangtse River Suspension Bridge with 1385 m-long main span in the completed stage, which is the longest-span bridge that has been constructed in China shown in Fig. 4, is performed as an actual example. The bridge deck section is a streamlined box with 36.9 m width and 3.0 m height (see Fig. 5) (Xiang *et al.* 1996).

A section model of the bridge deck with two degrees of freedom is used to measure flutter

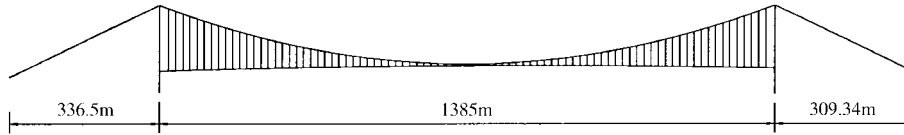


Fig. 4 Jiangyin Yangtse River Suspension Bridge

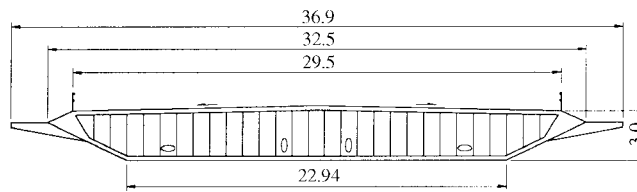


Fig. 5 Cross section of the bridge deck

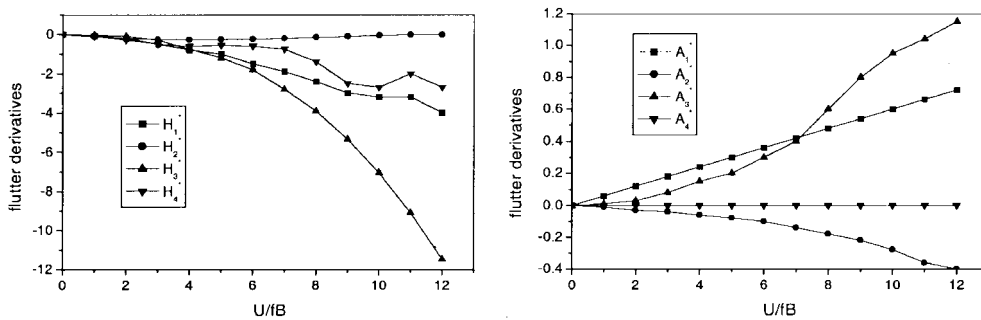


Fig. 6 Flutter derivatives H_i^* and A_i^* of the bridge deck

derivatives H_i^* and A_i^* ($i = 1 \sim 4$) in a wind tunnel; the results are shown in Fig. 6. The static lift, drag, and moment coefficients of the section at different angles of incidence are measured in laminar flow. The static coefficients of the deck section at zero degree of incidence are $C_L = 0.128$, $C_D = 0.0697$, $C_M = -0.0074$, $dC_L/d\alpha = -5.5577$, $dC_D/d\alpha = 0.0$, and $dC_M/d\alpha = 1.2662$. Since there is no measured result of flutter derivatives related to the lateral motion, these flutter derivatives are computed based on the quasi-steady theory. The structural damping ratio for each natural mode is assumed to be 0.005. To simplify the discussion of the fundamental characteristics of the buffeting response, only the aerodynamic forces acting on bridge deck are involved. The aerodynamic parameters are assumed to be uniform along the bridge axis, and the deformation due to the static wind is ignored.

The analytical model of the suspension bridge is established based on the design data. The first 50 natural modes are computed by the Lanczos method, and the major modes of the bridge deck are listed in Table 1. The Sturm check on the first 50 modes is conducted to prevent the missing of modes, and no mode is found missing.

The first 50 natural modes are taken into consideration in the buffeting response analysis. Fig. 7 indicates the effect of aerodynamic coupling among modes on the damping ratios of the first 15 complex modes as the reduced velocity increases. The solid lines and dashed lines are the results with and without coupling, respectively. It is noted that there are some significant difference in the

Table 1 Major modes of the bridge deck

No. Mode	Frequency (Hz)	Mode shape	No. Mode	Frequency (Hz)	Mode shape
1	0.0516	S-L	15	0.2730	S-T
2	0.0891	A-V	16	0.3107	A-V
3	0.1237	A-L	27	0.3707	S-V
4	0.1316	A-V	30	0.4132	S-T
5	0.1338	S-V	31	0.4322	A-V
6	0.1883	S-V	36	0.4990	S-V
7	0.2005	A-V	38	0.5304	A-T
12	0.2468	S-L	41	0.5690	A-V
13	0.2583	S-V	44	0.6444	S-V
14	0.2677	A-T	45	0.6640	S-T

Note: S - Symmetric; A - Antisymmetric; V - Vertical; L - Lateral; T - Torsional

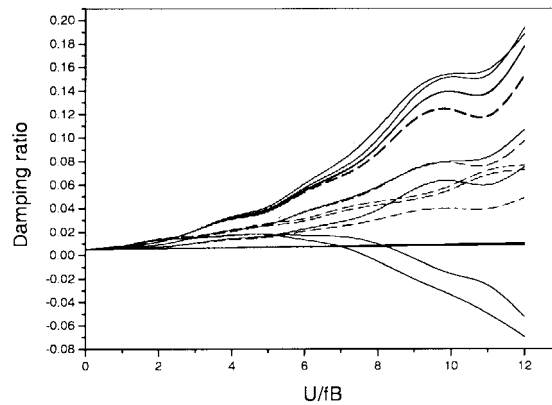


Fig. 7 Damping ratios versus reduced wind velocity (— with coupling; ---- without coupling)

vertical and torsional modes of the bridge structure.

The elevation z of the bridge deck at the main span center above ground is 60 m and the length z_0 of surface roughness is 0.01 m. To compute the buffeting responses in the interesting frequency range, a frequency interval about 0.002 is used within the range from 0.035 to 0.80 Hz. The aerodynamic admittance function of the bridge is not considered due to the lack of information. The power spectral densities of the displacement responses at the main span center are shown in Fig. 8 at a mean wind velocity of 60 m/s. The solid lines and dashed lines indicate the results by the present CQC method and by the conventional SRSS method, respectively. It has been noted that there are some difference near the first-order frequency for the PSDs of the vertical and torsional displacement responses due to the intermode effects. Furthermore, to illustrate the multimode effects on the buffeting response, the results with single mode are also included in the figures. It can be seen that for the suspension bridge, the multimode effects are significant for the PSDs of the buffeting displacement.

Fig. 9 shows the RMS values of the displacement responses at the main-span center with the mean wind velocity. It can be seen that the buffeting responses of vertical and torsional motions will

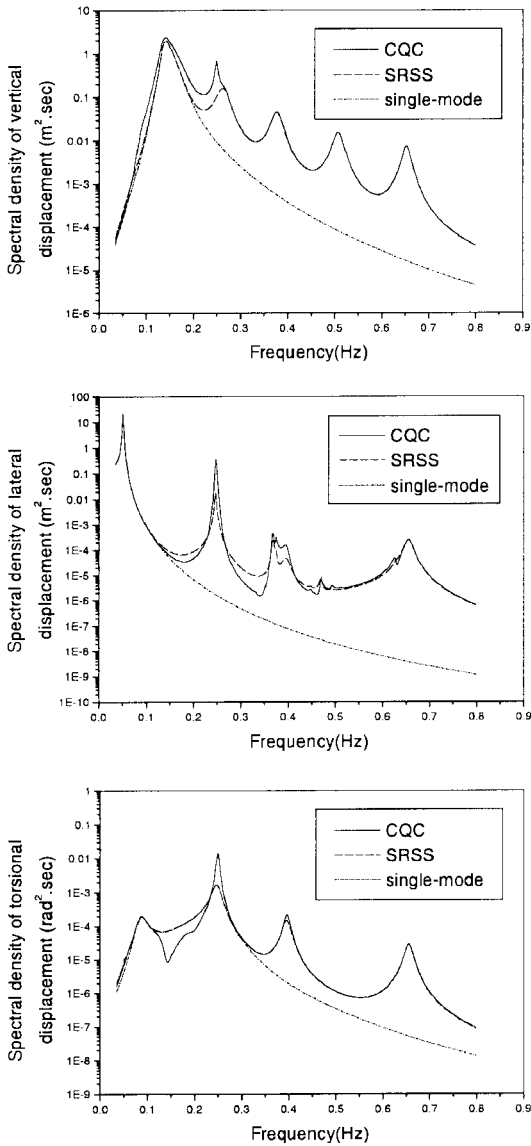


Fig. 8 PSDs of displacement responses at the main-span center

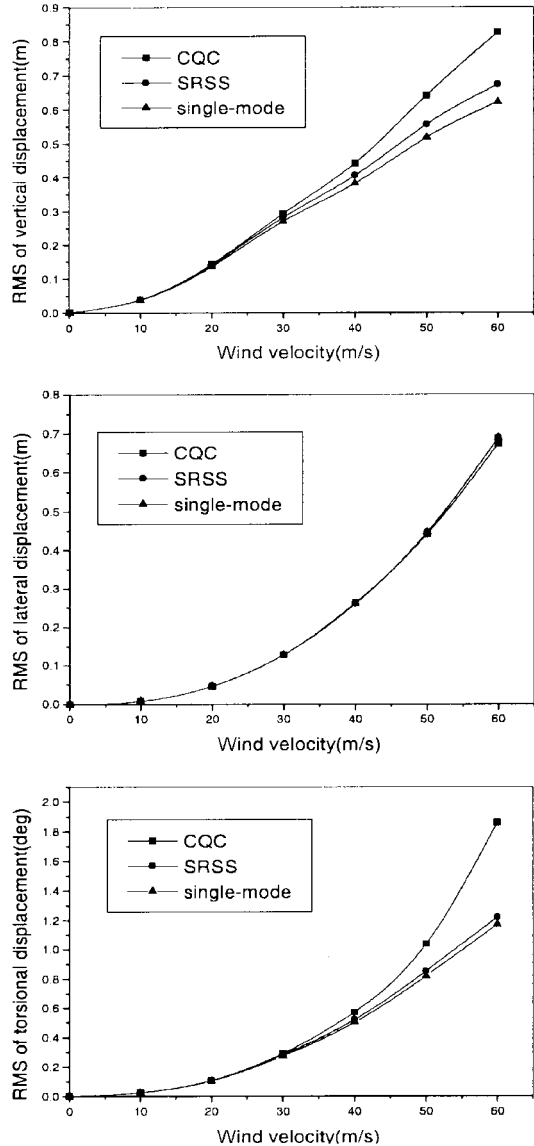


Fig. 9 RMS values of displacement responses at the main-span center

be underestimated using the single-mode analysis due to multimode and intermode effects. The difference between the CQC results and the SRSS ones is very small for the RMS responses of lateral displacement. However, the RMS response of vertical and torsional motions will be significantly underestimated using the conventional SRSS method, particularly at higher wind velocities. At the design wind velocity of 40 m/s, the RMS values of vertical and torsional displacements by the CQC method presented are 0.442 m and 0.573 deg, respectively. The corresponding results by the SRSS method are 0.405 m and 0.521 deg, which are 8.4% and 9.1%

smaller than the CQC results, respectively. Moreover, the corresponding results of the single-mode analysis are 0.382 m and 0.50 deg, which are 13.6% and 12.7% smaller than the CQC results, respectively.

In order to examine the influence of the CSDs of the generalized buffeting forces on the coupled buffeting responses, Eq. (30) excluding the influence is used. The RMS values of the buffeting responses of the vertical, lateral, and torsional displacement at the main-span center are 0.387 m, 0.2617 m, and 0.59 deg, respectively. Although these lateral and torsional displacement responses are slightly different from those including the CSDs of the generalized buffeting forces, there is significant difference for the vertical displacement response. Therefore, the influence on the coupled buffeting responses of long-span bridges due to the CSDs of the generalized buffeting forces can not be neglected. Furthermore, the writers have drawn the same conclusion by Scanlan's method. However, this conclusion is different from that provided by Chen (2000).

The cross spectra between the longitudinal and vertical wind fluctuations are neglected in the buffeting analysis aforementioned. However, if the real atmospheric turbulence is considered this assumption is not always conservative. Preliminary studies by Jones *et al.* (1992) indicated a 7% underestimate in buffeting response as a result of neglecting the wind cross spectrum in one instance. Another study (Attou 1993) demonstrated a 25% underestimate of the response due to the exclusion of the wind cross spectrum. Here a comparison study is performed for the suspension bridge.

Fig. 10 shows the comparison of the RMS values of displacement responses at the main-span

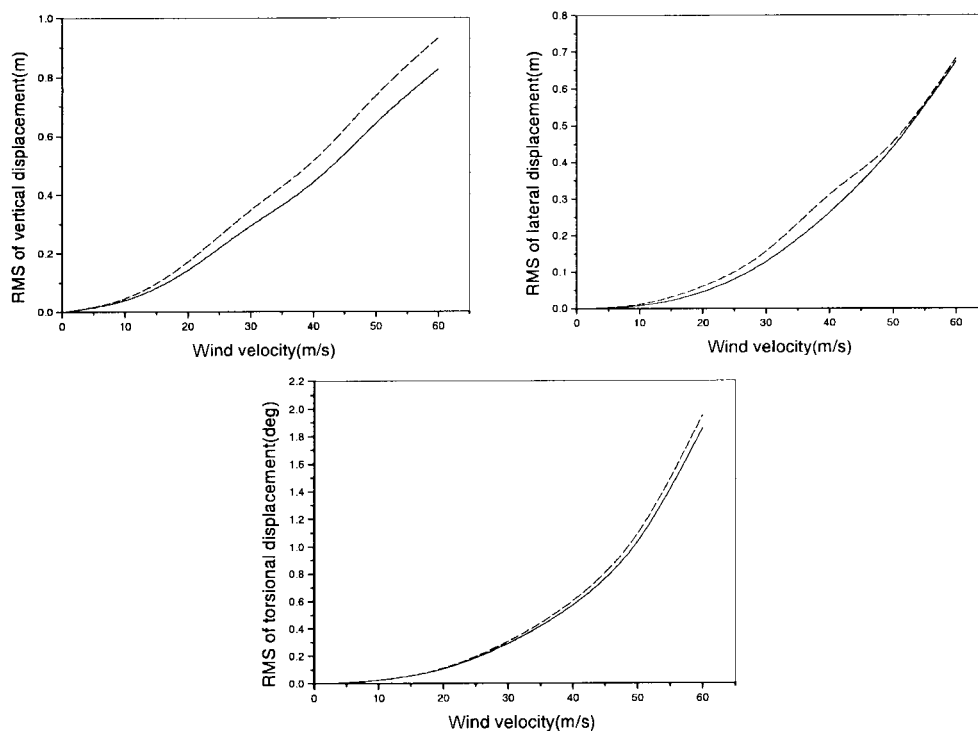


Fig. 10 RMS values of displacement responses at the main-span center with (---) and without (—) the wind cross spectrum

center with and without the wind cross spectrum. It has been noted that there are some significant difference between the two sets of results. The RMS values of the vertical, lateral, and torsional displacement responses at the main-span center are 0.442 m, 0.262 m, and 0.573 deg, respectively, excluding the wind cross spectrum at the mean wind velocity of 40 m/s. However, the corresponding results including the wind cross spectrum are 0.515 m, 0.311 m, and 0.603 deg, 16.5%, 18.7%, and 5.2% more, respectively.

5. Conclusions

Based on the modal coordinates of the structure, the finite-element and CQC method for analyzing the coupled buffeting response of long-span bridges is presented in this paper. The formulation of nodal equivalent aerodynamic buffeting forces is derived based on a reasonable assumption. The methodology for computing the power spectral density and variance of nodal displacements and elemental internal forces of bridge structures is presented using the finite-element method and the random vibration theory. The method presented is very efficient and can consider the arbitrary spectrum and spatial coherence of natural winds and the multimode and intermode effects on the buffeting responses of bridge structures.

To illustrate the reliability and effectiveness of the method presented and the associated analyzing software, the coupled buffeting problem of a simply supported beam structure is chosen as a check example. It has been noted that the results of the present method have very good agreement with those of Scanlan's method.

The coupled buffeting analysis of the Jiangyin Yangtse River Suspension Bridge with 1385 m main span is performed. The results of analysis show that the aerodynamic coupling among the vibration modes markedly affects the damping ratios of complex modes of the system. The multimode effects on the vertical and torsional displacement responses of the bridge deck are quite remarkable for the long-span suspension bridge. It is noted that there are some differences near the first-order frequency for the PSD of the vertical and torsional displacement responses due to the intermode effects. The RMS response of vertical and torsional motions will be significantly underestimated using the conventional SRSS method, particularly at higher wind velocities. At the design wind velocity of 40 m/s, the RMS responses of vertical and torsional displacements with the SRSS method are 8.4% and 9.1% smaller than the CQC results, respectively. Furthermore, the corresponding results of the single-mode analysis are 13.6% and 12.7% smaller than the CQC results. The influence on the coupled buffeting responses of long-span bridges due to the CSDs of generalized buffeting forces should not be neglected. Moreover, the cross spectra between the longitudinal and vertical wind fluctuations have obvious effects on the buffeting responses for this suspension bridge at the wind velocity of design and should be considered in its future study.

Acknowledgements

This paper is part of a large research project financially supported by the National Natural Science Foundation (NNSF) of China (Grants 59895410), which is gratefully acknowledged.

References

- Attou, M. (1993), "A computer program for the evaluation of dynamic response of structures to wind turbulence", *Proc. 3rd Asia-Pacific Symp. on Wind Engrg.*, Univ. of Hong Kong, Hong Kong.
- Cao, Y.H. (1999), "Nonlinear flutter and buffeting analysis in time domain for long-span bridges", Ph.D Dissertation of Tongji University, (in chinese).
- Chen, X., Matsumoto, M. and Kareem, A. (2000), "Time domain flutter and buffeting response analysis of bridges", *J. Engrg. Mech.*, ASCE, **126**(1), 7-16.
- Chen, X., Matsumoto, M. and Kareem, A. (2000), "Aerodynamic coupled effects on flutter and buffeting of bridges", *J. Engrg. Mech.*, ASCE, **126**(1), 17-26.
- Chen, W. (1993), "Study on buffeting response spectrum of long-span bridges", Ph.D Dissertation of Tongji University, (in chineses).
- Davenport, A.G. (1961), "The application of statistical concepts to the wind loading of structures", *Proc ICE*, **19**, 449-472.
- Davenport, A.G. (1962), "Buffeting of a suspension bridge by storm winds", *J. Struct. Engrg. Div.*, ASCE, **88**(6), 233-264.
- Jain, A., Jones, N.P. and Scanlan, R.H. (1996), "Coupled flutter and buffeting analysis of long-span bridges", *J. Struct. Engrg.*, ASCE, **122**(7), 716-725.
- Jones, N.P., Jain, A. and Scanlan, R.H. (1992), "Wind cross-spectrum effects on long-span bridges", *Proc. Engrg. Mech. Spec. Conf.* ASCE, New York.
- Kaimal, J.C. *et al.* (1972), "Spectral characteristics of surface-layer turbulence", *Quarterly J. Royal Meteorological Society*, Bracknell, England **98**, 563-589.
- Katsuchi, H., Jones, N.P. and Scanlan, R.H. (1999), "Multimode coupled flutter and buffeting analysis of the Akashi-Kaikyo bridge", *J. Struct. Engrg.*, ASCE, **125**(1), 60-70.
- Matsumoto, M., Chen, X. and Shiraishi, N. (1994), "Buffeting analysis of long-span bridge with aerodynamic coupling", *Proc. 13th National Symp. on Wind Engrg.*, Japan Association for Wind Engineering, 227-232 (in Japanese).
- Minh, N.N., Miyata, T., Yamada, H. and Sanada, Y. (1999), "Numerical simulation of wind turbulence and buffeting analysis of long-span bridges", *J. Wind Engineering & Industrial Aerodynamics*, **83**, 301-315.
- Panofsky, H.A. and Dutton, J.A. (1984), *Atmospheric Turbulence*, New York: John Wiley & Sons.
- Scanlan, R.H. and Gade, R.H. (1977), "Motion of suspended bridge spans under gusty wind", *J. Struct. Engrg. Div.*, ASCE, **103**(9), 1867-1883.
- Scanlan, R.H. (1978), "The action of flexible bridges under wind, II: buffeting theory", *J. Sound Vib.*, **60**(2), 201-211.
- Scanlan, R.H. and Jones, N.P. (1990), "Aeroelastic analysis of cable-stayed bridges", *J. Struct. Engrg.*, ASCE, **116**(2), 229-297.
- Scanlan, R.H. (1993), "Problematic in formulation of wind-force model for bridge decks", *J. Struct. Engrg.*, ASCE, **119**(7), 1433-1446.
- Simiu, E. and Scanlan, R.H. (1986), *Wind Effects on Structures* (2nd Ed). New York: John Wiley & Sons.
- Starossek, U. (1998), "Complex notation in flutter analysis", *J. Struct. Engrg.*, ASCE, **124**(8), 975-977.
- Xiang, H. *et al.* (1996), "Investigations on the wind-resisted behavior of Jiangyin Yangtse Suspension Bridge", Bulletin of Laboratory of Wind tunnel, SKLDRCE, Tongji Univ., Shanghai, China, (in chinese).
- Xu, Y.L., Sun, D.K., Ko, J.M. and Lin, J.H. (1998), "Buffeting analysis of long-span bridges: a new algorithm", *Computers and Structures*, **68**, 303-313.